Journal of Non-Crystalline Solids, Volume 452, 15 November 2016, Pages 30-34
DOI:10.1016/j.jnoncrysol.2016.08.010

Accepted Manuscript
Non-Crystalline Solids
Received 13 June 2016
Revised 3 August 2016
Accepted 5 August 2016
https://doi.org/10.1016/j.jnoncrysol.2016.08.010

In-situ structural identification of Zr_3Al_2 type metastable phase during crystallization of a Zr-based MG

Yan Xing[a], Yan Li[a,*], Xiangke Wang[a], Xiangtian Yu[a], Tao Zhang[b], Konstantinos Georgarakis[c]

[a] *China Aerospace Components Engineering Center, China Academy of Space Technology, Beijing 100094, China*

[b] *Key Laboratory of Aerospace Materials and Performance (Ministry of Education), School of Materials Science and Engineering, Beihang University, Beijing 100191, China*

[c] *Euronanao, SIMap-LTPCM, Institut Polytechnique de Grenoble INPG, BP 75, Saint-Martin-d'Heres Campus 38402, France*

Abstract:

A metastable phase was detected using higher energy synchrotron radiation when Zr-based metallic glass (MG) was annealed under vacuum in Linkam hot stage at 848 K. The formation and transformation processes of metastable phase were recorded by synchrotron radiation method. The metastable phase during crystallization was identified as Zr_3Al_2 structure type according to powder diffraction and TEM analysis. The structure of Zr_3Al_2 type MCP was experimentally evidenced by 3D diffraction patterns and mathematically described. The identification of Zr_3Al_2 MCP could be helpful for the understanding of cluster structure of MG.

Key Words:
metallic glass, metastable phase, crystallization, synchrotron radiation

**Corresponding author: Yan Li (liyan1123@126.com)*

1 Introduction

Metallic glasses (MGs) have drawn great attention because of their unique liquid-like structure and the combination of superior properties, including high yield strength, good elasticity, good magnetic properties, high wear resistance and high corrosion resistance [1-3]. Upon heating, MGs undergo a series of thermal events including glass transition temperature (T_g), supercooled liquid region (ΔT_x) and crystallization temperature (T_x). In several MG systems, it has been reported previously that the crystallization process leads to the formation of distinctive metastable structures, such metastable crystalline phase (MCP) and metastable quasicrystal phase (MQC), as a result of nucleation of crystals from the non-equilibrium amorphous matrix [4-7]. Previous findings revealed the formation of MCP in $Zr_{55}Al_{10}Ni_5Cu_{30}$ MG [6] and MQCs in $Zr_{63}Cu_{25}Al_{12}$, $Zr_{65}Cu_{17.5}Ni_{10}Al_{7.5}$ and $Zr_{69.5}Cu_{12}Ni_{11}Al_{7.5}$ alloys during heating [8]. Subsequently, a number of studies were reported that MCPs or icosahedral MQCs were formed in different Zr-based MGs. For example, MQCs were found in Zr-based binary, ternary and multicomponent metallic glass formers with the addition of Ti, Pd or Pt [9-11]. Using fast quenching or ion irradiation methods [12, 13], MCPs or MQCs were also observed in metallic glassy matrix. When 1 wt.% La_2O_3 was introduced into $Zr_{55}Al_{10}Ni_5Cu_{30}$ alloy, MCP and MQC coexisted after thermal treatment [14]. Recent publications concerning metastable and quasicrystal phases formed in Zr-based glassy matrix are listed in table 1, which summarizes compositions or composition range of MCP/MQC formers, formation methods and the structure type of metastable phases.

In addition to alloy composition factor, oxygen impurity in the alloy, which can be introduced from raw materials or annealing environment, were also found to affect the nucleation process of

metastable phases in Zr-based alloys [30, 34]. When the content of oxygen reached 4.3 atomic percent (at.%) in $Zr_{65}Cu_{27.5}Al_{7.5}$ ternary alloy, MQC had precipitated from glassy matrix [30]. However, when the content was lower than the critical value, another stable crystalline phase instead of MQC appeared. Similar experimental results were demonstrated in another study that high content of oxygen promoted the crystallization of metastable phase via the redistribution of oxygen [34]. Due to the different fabrication environment of MGs, the precipitation of MQCs in $Zr_{65}Cu_{17.5}Ni_{10}Al_{7.5}$ and $Zr_{69.5}Cu_{12}Ni_{11}Al_{7.5}$ MGs indicating low reproducible reliability which also can be interpreted by the different contents of oxygen. More recent researches interpreted the crystallization mechanisms in the point of view of thermodynamics and kinetics [37, 38].

In terms of MCP formation in MGs, the same one was found to have nucleated from the glassy matrix in annealed $Zr_{55}Al_{10}Ni_5Cu_{30}$, $Zr_{55}Cu_{20}Al_{10}Ni_{10}Pd_5$ and some other Zr-based MGs according to previous studies [15, 16]. The accurate identification of MCP structure is important because that it could be a strong evidence to interpret the configuration of clusters of metallic glasses. In order to clarify the structure of metastable crystalline phase of Zr-based MGs during crystallization, $Zr_{69.5}Cu_{12}Ni_{11}Al_{7.5}$ MG was adopted in our work for further investigation. In this work, using high energy synchrotron radiation in transmission mode during in-situ heating and transmission electron microscopy (TEM), the structure of MCP nucleated in $Zr_{69.5}Cu_{12}Ni_{11}Al_{7.5}$ metallic glass was identified and high temperature crystallization results were investigated.

2 Experimental

Master ingots of $Zr_{69.5}Cu_{12}Ni_{11}Al_{7.5}$ (at.%) alloy were prepared by arc melting using high purity

metals, which were melted more than 3 times for homogeneity under the protection of high purity argon. Glassy ribbons were synthesized by melt spinning method. The ribbons were annealed under vacuum in a thermal treatment furnace at 848 K and 1073 K, respectively.

The as-spun ribbons without annealing were sealed under protection of argon flow in quartz capillaries and placed on a computer-controlled Linkam hot stage. The temperature was well controlled below the melting temperature of Zr-based alloy to prevent the reaction between Zr and Si of quartz crucible. The in-situ heating samples were examined using high energy synchrotron radiation in transmission on the ID11 beam line of the European Synchrotron Radiation Facilities (ESRF), which was monochromatized using a nitrogen-cooled double crystal silicon monochromater. The photon energy was 80 keV corresponding to an X-ray wave-length (λ) of about 0.015498 nm. The diffraction spectra were acquired in transmission mode through the quartz capillary in the Linkam by a 2D CCD camera. The heating rate of the Linkam was 10 K/min. Acquisition and data processing times were configured as 20 seconds such that a full spectrum can be obtained.

The annealed samples were ground into the metallic powder. The powder was loaded into a thin glass capillary and mounted in a sample holder on the ID 31 high resolution powder diffractometer with the wave-length (λ) of 0.050002 nm. The structure of the sample annealed at 848 K was investigated by TEM using selected area electron diffraction (SAED) with the wave-length (λ) of 0.1542 nm.

3 Results and discussion

The X-ray diffraction patterns obtained under in-situ heating using synchrotron radiation in

transmission mode, the transition in detail from a metastable phase to stable ones, and the volume fractions of different nucleated crystalline phases as a function of temperature are shown in Fig. 1. In Fig. 1 a, $Zr_{69.5}Cu_{12}Ni_{11}Al_{7.5}$ alloy exhibit fully amorphous microstructure evidenced by the absence of sharp Bragg peaks corresponding to crystalline structures, until the temperature reached T_x (~763 K). The phase initially nucleated from the amorphous alloy can be identified as a metastable phase. When the temperature went higher than 950 K, the peaks of the metastable crystalline phase was disappeared in Fig. 1 a. The phase transition from the metastable phase to stable ones can be clearly observed from Fig. 1 b, which is an enlarged view of Fig. 1 a. The diffraction peaks of disappearing metastable phase and emerging stable ones are marked in Fig. 1 b. The intensity of metastable phase was decreasing with the increase of temperature and the peaks disappear when the temperature reaches about 978 K. From Fig.1a and Fig1.1b, it appears that the strongest peak of the metastable phase has not vanished completely. However, the peak is shared by the bcc Zr phase, as are many similar peaks in the diffraction pattern.

The stable phases transform from metastable and the new crystalline particles significantly grow in the temperature region of that of diminishing of metastable phase. The volume of each crystalline phase was normalized using the following formula:

$$V_f = \frac{ph\_frac_i V_{uc_i}}{\sum_{i=1}^{N} ph\_frac_i V_{uc_i}} \quad (1)$$

where $ph\_frac_i V_{uc_i}$ is the phase fraction of phase *i* and V_{uc_i} is the volume of the unit cell of that phase. In Fig. 1 c, the metastable phase (marked with solid triangle) nucleated at ~790 K, followed by bcc Zr (marked with cross). The volume fraction of MCP decreased from ~0.42 to 0 when the temperature went up from ~890 K to ~990 K. The stable phases including Zr_6NiAl_2)

(marked by solid square) and Zr_2Cu (marked with solid diamond) nucleated at about 850 K and 875 K, respectively.

Fig. 2 presents the diffraction pattern of annealed sample at 848 K (marked with black solid squares) using high energy powder X-ray diffractometer. In order to identify the structures of the crystalline phases, a thorough search of a database known as the Pauling Files [39] was made. The structures of all known binary combinations of the four elements zirconium, copper, nickel and aluminum were saved. The program "Powdercell" [40] was used to display the calculated diffraction patterns of these binaries. These are superimposed on top of the diffraction pattern from ID31. The calculated Zr_3Al_2 and bcc Zr crystalline phase diffraction patterns match very well with the observed pattern of annealed $Zr_{69.5}Cu_{12}Ni_{11}Al_{7.5}$ alloy. A Zr_3Al_2 type structure can be identified for the metastable crystalline phase as marked with solid triangle. In the meantime, bcc Zr can also be observed with very similar diffraction peak positions to those of Zr_3Al_2.

When the temperature increased, the transformation from Zr_3Al_2 MCP to stable phases occurred, as shown in Fig. 1. The crystalline phases annealed at 1073 K were identified using powder diffraction in ID31. The experimental diffraction patterns and the ones form database were compared in Fig 3. The annealed alloy is composed of multi-crystalline stable phases, which include bcc Zr, Zr_2Cu and ternary intermetallic Zr_6NiAl_2. In contrast, there is a complete absence of Zr_3Al_2 structure type metastable phase in the XRD diffraction pattern. From Fig.1, Fig. 2 and Fig. 3, the whole crystallization process and products are summarized in following equation:

$$Amorphous\_Phase \xrightarrow{763K} Zr_3Al_2\_MCP + bcc\_Zr + remaining\_Amor \xrightarrow{880K}$$
$$Zr_3Al_2\_MCP + bcc\_Zr + Zr_2Cu + Zr_6NiAl_2 \xrightarrow{950K} bcc\_Zr + Zr_2Cu + Zr_6NiAl_2$$

The Zr_3Al_2 structure type metastable phase exhibits good thermal stability, which was observed in $Zr_{55}Al_{10}Ni_5Cu_{30}$ and $Zr_{55}Cu_{20}Al_{10}Ni_{10}Pd_5$ annealed alloys [15, 18]. The ratio of

transformation temperature over melting temperature is about 0.913. From previous results [15], the annealing temperature of Zr_3Al_2 metastable phase is identified at nearly up to the melting point under fast heating rate. The difference in thermal stability of MCPs could be affected by heating rates and impurities. When the oxygen content goes up to 0.43 at.% [30], the formation of icosahedral quasicrystal phase nucleates instead of Zr_3Al_2 structure type MCP. The variability of MCP and MQC can be interpreted by the affinity of Zr and O and when oxygen concentration reaches critical value. The formation of MCP and MQC was also found to be accompanied by the redistribution of oxygen [30, 34].

Using TEM and selected area electron diffraction (SAED), the structure of Zr_3Al_2 structure type MCP was confirmed. Fig. 4 shows SAED patterns corresponding to three different crystallographic zone axes. The MCP is a tetragonal structured crystal with lattice parameters a =7.88(±0.08) Å and c =7.10(±0.08) Å. To visualize the crystal structure, the 3D crystal structure image was built and demonstrated in Fig. 5 using “Diamond” method [41]. The structure model is composed of large blue balls and small white ones, representing Zr/Ni/Cu and Al/Ni/Cu atoms, respectively. This means that Ni and Cu are capable of potentially occupying both ball positions. However, taking in to the consideration that the atomic percentage of Zr in $Zr_{69.5}Cu_{12}Ni_{11}Al_{7.5}$ alloy and Zr_3Al_2 MCP, and the atomic radii differences between Zr and M (Ni, Cu and Al), it is more probable that Zr atoms reside at the positions of blue balls and M (Ni, Cu and Al) occupy the positions of white balls. Therefore, $Zr_3(Ni/Cu/Al)_2$ structure may be a reasonable structure of the metastable phase. As an intermediate stage between amorphous and Zr_2M (Zr_2Cu and Zr_6NiAl_2) type stable phases, study on the Zr_3Al_2 structure MCP with good thermal stability may benefit the understanding on the structure of multi-component Zr-based metallic glasses and their

devirtification behaviors.

In summary, the in-situ crystallization processes and the formation of metastable phase in $Zr_{69.5}Cu_{12}Ni_{11}Al_{7.5}$ metallic glass with low content of oxygen were observed and analyzed using high energy synchrotron radiation. The metastable phase during crystallization was found and the structure of MCP was identified as Zr_3Al_2 structure type according to powder diffraction and TEM analysis. The transition from Zr_3Al_2 type MCP to Zr_2Cu and Zr_6NiAl_2 was experimentally evidenced by 3D diffraction patterns and mathematically described using volume fraction function.

Acknowledgement

This work was financially supported by the National Nature Science Foundation of China (51305483). The ESRF are acknowledged for the experimental works using X-ray diffraction. We acknowledge the contributions of Dr. L. Huang for her helpful discussion and corrections. Yan Li and Konstantinos Georgarakis appreciate Professor Alain Reza Yavari for his edification.

References

[1] A. Inoue. Stabilization of metallic supercooled liquid and bulk amorphous alloys. Acta Mater. 48 (2000) 279-306.

[2] A. Inoue, T. Zhang and T. Masumoto, Al-La-Ni Amorphous Alloys with a Wide Supercooled Liquid Region. Mater. Trans., JIM. 30 (1989) 965-972.

[3] A. Peter, W. L. Johnson, A highly processable metallic glass: $Zr_{41.2}Ti_{13.8}Cu_{12.5}Ni_{10.0}Be_{22.5}$, Appl. Phys. Lett. 63 (1993) 2342-2344.

[4] A. Inoue. Amorphous, nanoquasicrystalline and nanocrystalline alloys in Al-based systems. Prog. Mater. Sci. 43 (1998) 365-520.

[5] I. T. Walker, A. L. Greer. Displacive transformations in Fe–Ni nanophase alloys. Mater. Sci. Eng. A, 304-306 (2001) 905-909.

[6] A.R. Yavari, A. Le Moulec, W.J. Botta F., A. Inoue, P. Rejmankova, A. Kvick. In situ crystallization of Zr55Cu30Al10Ni5 bulk glass forming from the glassy and undercooled liquid states using synchrotron radiation. J. Non-Cry. Solid, 247 (1999) 31-34.

[7] K. F. Kelton. Ti/Zr/Hf-based quasicrystals. Mater. Sci. Eng. A 375-377 (2004) 31-37.

[8] U. Koster, J. Meinhardt, S. Roos, H. Liebertz. Formation of quasicrystals in bulk glass forming Zr-Cu-Ni-Al alloys. Appl. Phys. Lett. 69, 2 (1996) 179-181.

[9] U. Kuhn, K. Eymann, N. Mattern, J. Eckert, A. Gebert, B. Bartusch, L. Schultz. Limited quasicrystal formation in Zr-Ti-Cu-Ni-Al bulk metallic glasses. Acta Mater. 54 (2006) 4685-4692.

[10] T. Zhang, A. Inoue, M. Matsushita, J. Saida. Formation of icosahedral quasicrystal by crystallization of Zr70(Ni, Cu, Pd)30 amorphous alloys. J. Mater. Res., 16, 1 (2001) 20-23.

[11] M.H. Lee, R.T. Ott, M.F. Besser, M.J. Kramer, D.J. Sordelet. CoMCPositional dependence on phase selection during devitrification of amorphous Zr-Pt alloys. Scripta Mater. 55 (2006) 505-508.

[12] S. Nagata, S. Higashi, B. Tsuchiya, K. Toh, T. Shikama, K. Takahiro, K. Ozaki, K. Kawatusra, S. Yamamoto, A Inouye. Ion irradiation effects on amorphization and thermal crystallization in Zr-Al-Ni-Cu alloys. Nucl. Instr. and Meth in Phys. Res. B 257 (2007) 420-423.

[13] J.B. Qiang, W. Zhang, G.Q. Xie, A. Inoue. Effect of Ti addition on the crystallization behavior and glass-forming ability of Zr-Al-Cu alloys. J. Non-Cry. Solid, 354 (2008) 2054-2059.

[14] M.F. de Oliveira, C.S. Kiminami, W.J. Botta F. Effect of oxide particles on the crystallization behavior of Zr55Al10Ni5Cu30 alloy. Mater. Sci. Eng. A 304-306 (2001) 665-669.

[15] A.R. Yavari, A. Le Moulec, A. Inoue, W.J. Botta F., G. Vaughan, A. Kvick. Metastable phases in Zr-based bulk glass-forming alloys detected using a synchrotron beam in transmission. Mater. Sci. Eng. A, 304-306 (2001) 34-38.

[16] A.R. Yavari, A. Inoue, T. Zhang, W.J. Botta F., A. Kvick. Metastable phases, quasicrystals and solid solutions in Zr-based bulk glass-forming alloys. Scripta Mater. 44 (2001) 1239-1244.

[17] L.C. Damonte, L.A. Mendoza-Zelis, S. Deledda, J. Eckert. Effect of preparation conditions on the short-range order in Zr-based bulk glass-forming alloys. Mater. Sci. Eng. A 343 (2003) 194-198.

[18] J.L. Uriarte, T. Zhang, S. Deledda, G. Vaughan, A.R. Yavari, A. Inoue, A. Kvick. Real-time detection of metastable phases in Zr-based bulk glasses during fast heating in a synchrotron

beam. J. Non-Cry. Solid, 287 (2001) 197-200.

[19] B.S. Murty, D.H. Ping, M. Ohnuma, K. Hono. Nanoquasicrystalline phase formation in binary Zr-Pd and Zr-Pt alloys. Acta Mater. 49 (2001) 3453-3462.

[20] M.S. El-Eskandarany, J. Saida, A. Inoue. Amorphization and crystallization behaviors of glassy Zr70Pd30 alloys prepared by different techniques. Acta Mater. 50 (2002) 2725-2736.

[21] B.S. Murty, D.H. Ping, K. Hono. Nanoquasicrystallization of binary Zr-Pd metallic glasses. Appl. Phys. Lett. 77, 8 (2000) 1102-1104.

[22] J.R. Morris, Min Xu, Y.Y. Ye, D.J. Sordelet, M.J. Kramer. Theoretical and experimental studies of devitrification pathways in the Zr2Cu1-xPdx metallic glass system. Acta Mater. 55 (2007) 5901-5909.

[23] C.F. Li, A. Inoue. Precipitation of icosahedral quasicrystalline phase in metallic Zr65Al7.5Ni5Cu17.5Re5 glass. Mater. Lett. 50 (2001) 318-321.

[24] S. Scudino, S. Venkataraman, J. Eckert. Thermal stability, microstructure and crystallizations kinetics of melt-spun Zr-Ti-Cu-Ni metallic glass. J. Alloy CoMCPd. 460 (2008) 263-267.

[25] C.F. Li, L.M. Wang, A. Inoue. Precipitation of icosahedral quasicrystalline and crystalline approximant phases in Zr-Cu-(Co, Ph, or Ir) metallic glasses. J. Non-Cry. Solid, 306 (2002) 175-181.

[26] S. Scudino, J. Eckert, H. Breitzke, K. Luders, L. Schultz. Effect of Zr on the crystalline behavior of multi-coMCPonent Zr-based metallic glasses. J. Alloy CoMCPd. 434-435 (2007) 217-220.

[27] C.F. Li, A. Inoue. Effect of Zn on the crystallization process in $Zr_{65}Al_{7.5}Ni_{10}Cu_{17.5}$ metallic glass. J. Alloy CoMCPd. 325 (2001) 230-235.

[28] T. Nagase, T. Hosokawa, Y. Umakoshi. Electron irradiation induced phase transformation in $Zr_{66.7}Cu_{33.3}$ and $Z_{r66.7}Pd_{33.3}$ metallic glass. Scripta Mater. 53 (2005) 1401-1405.

[29] L.C. Damonte, L. Mendoza-Zelis. Crystallization steps in Zr- and Hf-based bulk metallic glasses. J. Alloy CoMCPd. 434-435 (2007) 244-247.

[30] B.S. Murty, D.H. Ping, K. Hono. Direct evidence for oxygen stabilization of icosahedral phase during crystallization of Zr65Cu27.5Al7.5 metallic glass. Appl. Phys. Lett. 76, 1 (2000) 55-57.

[31] M. Yan, J. Zou, J. Shen. A TEM study on the crystallization behavior of an yttrium-doped Zr-based bulk metallic glass. Intermetallics 15 (2007) 961-967.

[32] L.M. Wang, C.F. Li, L.Q. Ma, A. Inoue. Formation of Zr70Ni23Ti7 glassy alloy and phase transformation upon heating. J. Mater. Res. 17, 3 (2002) 693-696.

[33] R. Allen, G. L'Esperance, Z. Altounian, J.O. Strom-Olsen. A TEM study of the microstructures formed during the crystallization of Ni-Zr metallic glasses. J. Mater. Res. 6, 4 (1991) 755-759.

[34] M.W. Chen, A Inoue, T. Sakurai, D.H. Ping, K. Hono. IMCPurity oxygen redistribution in a nanocrystallized Zr65Cr15Al10Pd10 metallic glass. Appl. Phys. Lett. 74, 6 (1999) 812-814.

[35] J. Gubicza, J.L. Labar, E. Agocs, D. Fatay, J. Lendvai. Effect of nano-quasicrystals on viscosity of a Zr-based bulk metallic glass. Scripta Mater. 58 (2008) 291-294.

[36] X. Zhao, C. Ma, S. Pang, T. Zhang. Glass-forming ability and I-phase formation in Y-doped Zr-Nb-Ni-Al glassy alloys. Philosophical Magazine Letters, 89 (2009) 11-18.

[37] Y.H. Li, C. Yang, L.M. Kang, H.D. Zhao, S.G. Qu, X.Q. Li, W.W. Zhang, Y.Y. Li. Non-isothermal and isothermal crystallization kinetics and their effect on microstructure of

sintered and crystallized TiNbZrTaSi bulk alloys. Journal of Non-crystalline Solids, 432 (2016) 440-452.

[38] C. Yang, L.H. Liu, Y.G. Yao, Y.H. Li, Y.Y. Li. Intrinsic relationship between crystallization mechanism of metallic glass powder and microstructure of bulk alloys fabricated by powder consolidation and crystallization of amorphous phase. Journal of Alloys and Compounds, 586 (2014) 542-548.

[39] P. Villars. Pauling Files Binary Edition. Version 1.0, 2002

[40] W. Kraus, G. Nolze. J. Appl. Cryst. 29 (1996) 301-303.

[41] W.Massa. Crystal Structure Determination. Springer-Verlag Berlin Heidelberg, 2000

Table 1

Table1 Metastable and quasicrystal phases in Zr-based metallic glasses

Alloys	Metastable phase	Method	References
$Zr_{55}Cu_{30}Al_{10}Ni_5$	MCP	annealing; ion irradiation	6, 14, 15, 16 12
$Zr_{55}Cu_{20}Al_{10}Ni_{10}Pd_5$	MCP	annealing	18
$Zr_{70}Pd_{30}$	MQC	annealing	10, 19, 20, 21
$Zr_{70}Ni_{30-x}Pd_x$, $Zr_{70}Cu_{30-x}Pd_x$ $Zr_{70}Ni_{10}Cu_{10}Pd_{10}$ (x=10, 20 at.%)	MQC	annealing	10
$Zr_{55}Ti_4Cu_{25}Al_{10}Cu_{16}$	MCP	annealing	15, 16
$Zr_{69.5}Cu_{12}Ni_{11}Al_{7.5}$	MCP MQC	annealing	15, 16, ***this work*** 8
$Zr_{65}Pd_{10}Al_{7.5}Ni_{10}Cu_{7.5}$	MQC	annealing	16
$Zr_2Cu_{0.5}Pd_{0.5}$	MQC (C16)	annealing	22
$Zr_{65}Al_{7.5}Ni_5Cu_{17.5}Re_5$	MQC	annealing	23
$Zr_{63.33}Ti_{8.89}Cu_{15.45}Ni_{12.33}$	MQC	annealing	24
$Zr_{62-x}Ti_xCu_{20}Ni_8Al_{10}$ ($2 \leq x < 4$)	MQC	annealing	9
$Zr_{65}Pd_{35}$, $Zr_{80}Pt_{20}$	MQC	annealing cooling	19, 21
$Zr_{70}Cu_{20}Ir_{10}$, $Zr_{70}Cu_{20}Rh_{10}$	MCP (Ti_2Ni type)	annealing	25
$Zr_y(Ti_{0.186}Nb_{0.058}Cu_{0.324}Ni_{0.258}Al_{0.174})_{100-y}$ (y=57 and 62)	MQC	annealing	26
$Zr_{65}Al_{7.5}Ni_5Cu_{17.5}Zn_5$	MQC	annealing	27
$Zr_{66.7}Pd_{33.3}$	MQC	annealing	28

$Zr_{52.5}Hf_2Ti_{7.5}Cu_{20}Al_{10}Ni_8$	MCP (Ti_2Ni-type)	annealing	17, 29
$Zr_{75}Pt_{25}$, $Zr_{77}Pt_{23}$	MQC	annealing	11
$Zr_{65-x}Cu_{27.5}Al_{7.5}O_x$ (x=0.43% and 0.82%)	MQC	annealing	30
$(Zr_{0.51}Cu_{0.207}Ni_{0.12}Al_{0.163})_{99.5}Y_{0.5}$	MCP (orthorhombic)	annealing	31
$Zr_{65}Ni_{17.5}Ni_{10}Al_{7.5}$	MQC	annealing	8
$Zr_{70}Ni_{23}Ti_7$	MQC	annealing	32
$Zr_{67}Ni_{33}$, $Zr_{58}Ni_{42}$	MCP	annealing	33
$Zr_{65}Cr_{15}Al_{10}Pd_{10}$	MCP (O-rich)	annealing	34
$(Zr_{65}Al_{7.5}Cu_{27.5})_{100-x}Ti_x$ (x=2-15 at.%) $(Zr_{65}Al_{7.5}Cu_{27.5})_{90}Ti_{10}$	MQC	annealing as cast	13
$Zr_{55}Al_{10}Ni_5Cu_{30}$ +1 wt.% La_2O_3	MCP+MQC	annealing	14
$Zr_{44}Ti_{11}Cu_{10}Ni_{10}Be_{25}$	MQC	annealing	35
$(Zr_{0.58}Nb_{0.03}Cu_{0.16}Ni_{0.13}Al_{0.1})_{98.5}Y_{1.5}$	MQC	annealing	36

List of figures

Figure
Click here to download high resolution image

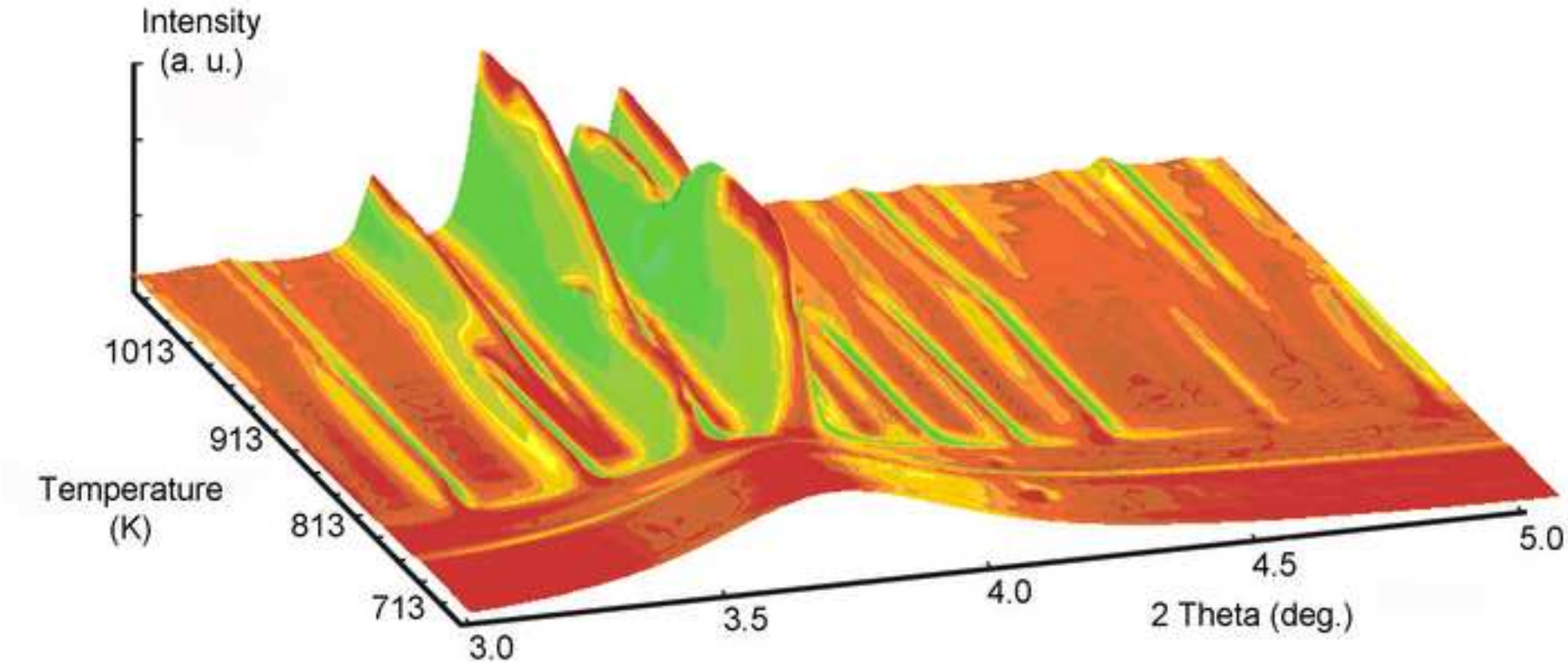

Figure
Click here to download high resolution image

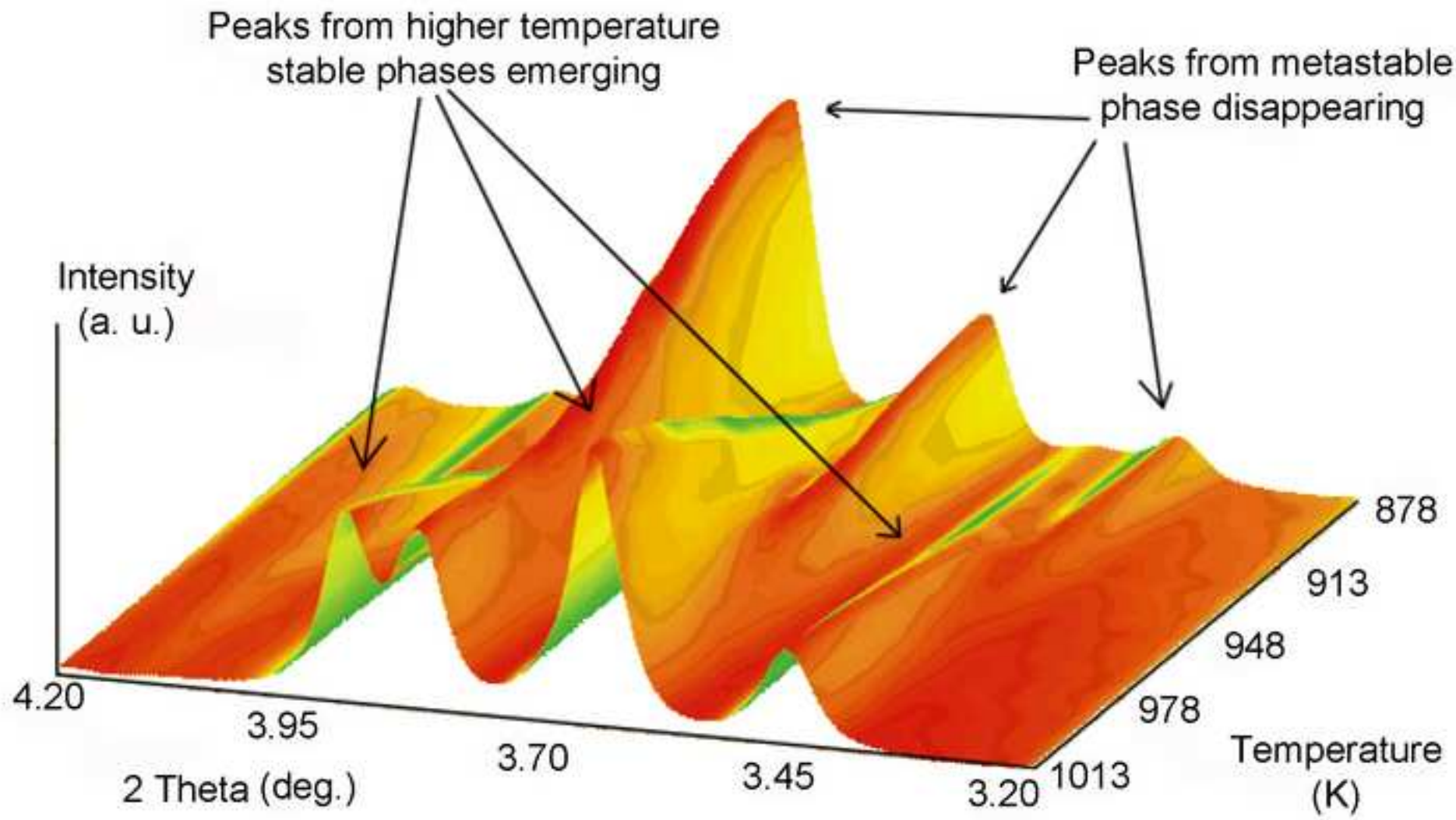

Figure

Click here to download high resolution image

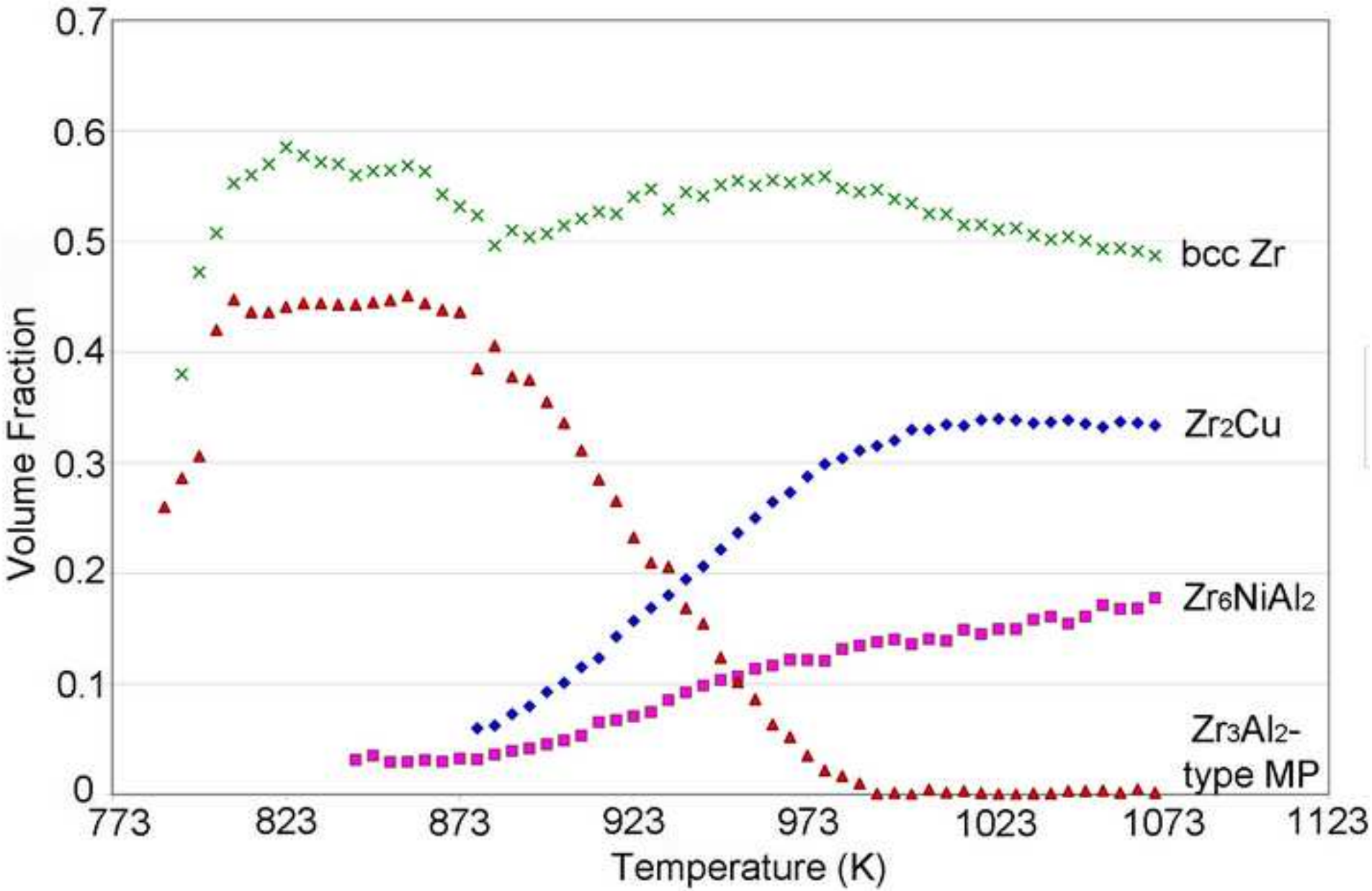

Figure

Click here to download high resolution image

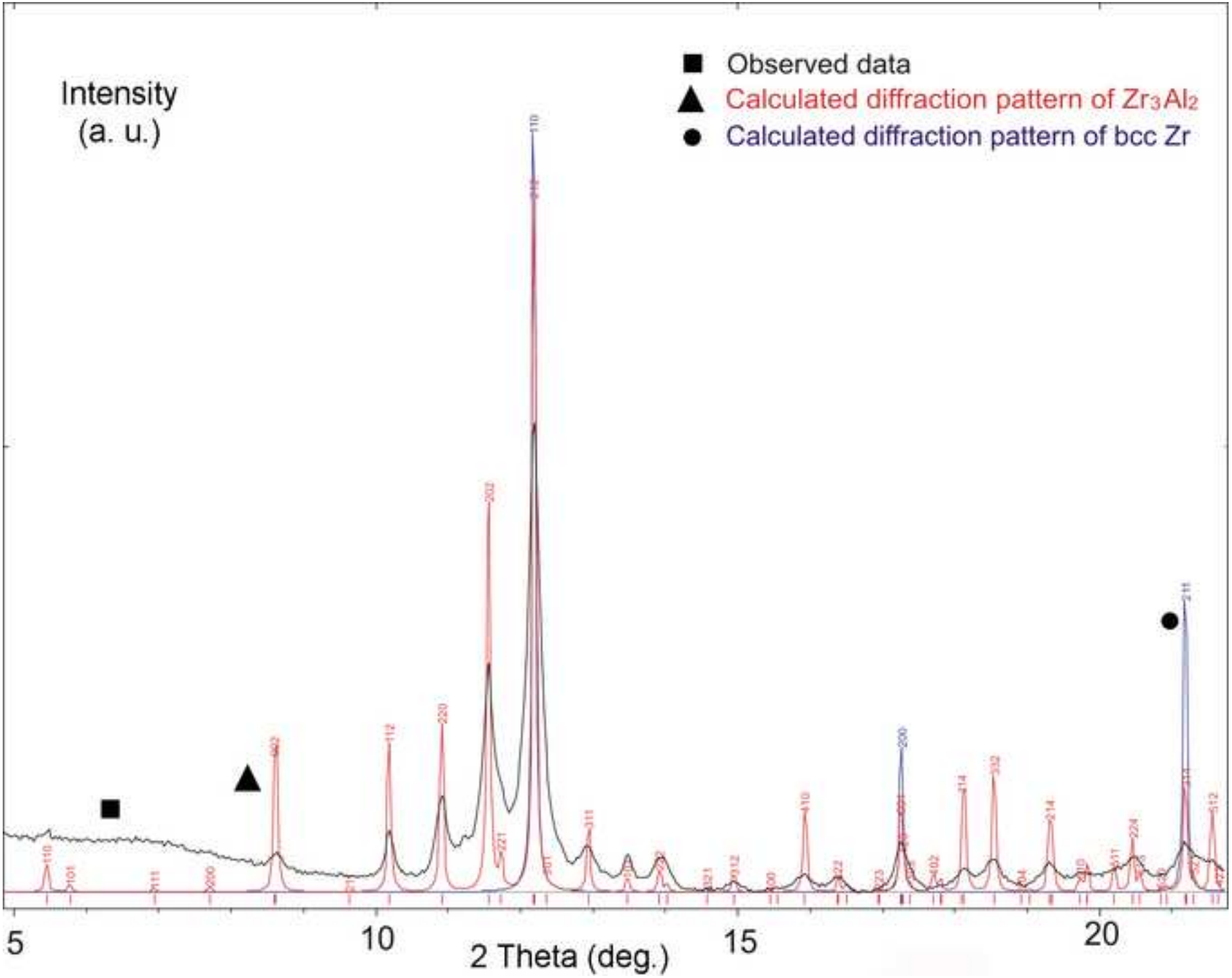

Figure

Click here to download high resolution image

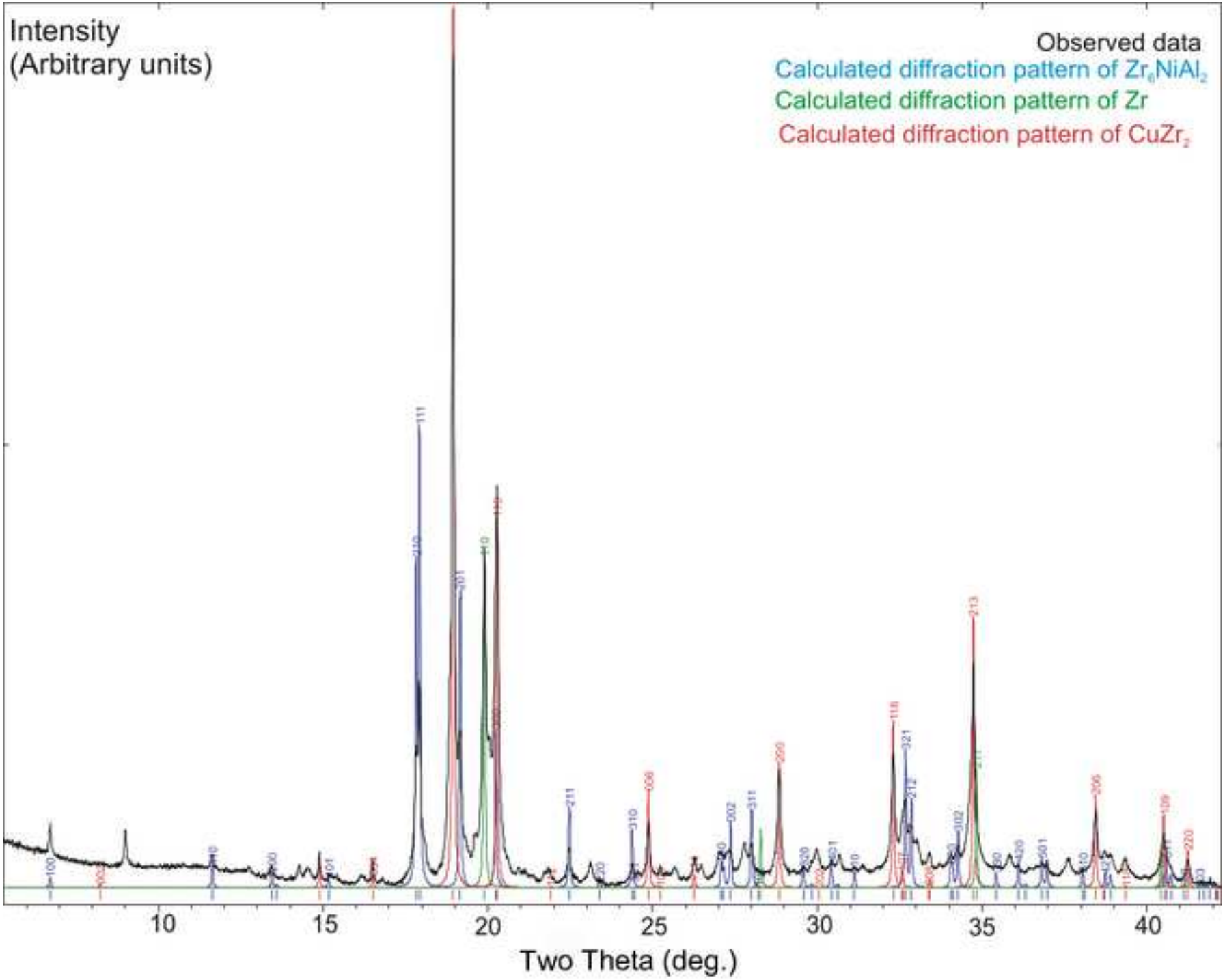

Figure

Click here to download high resolution image

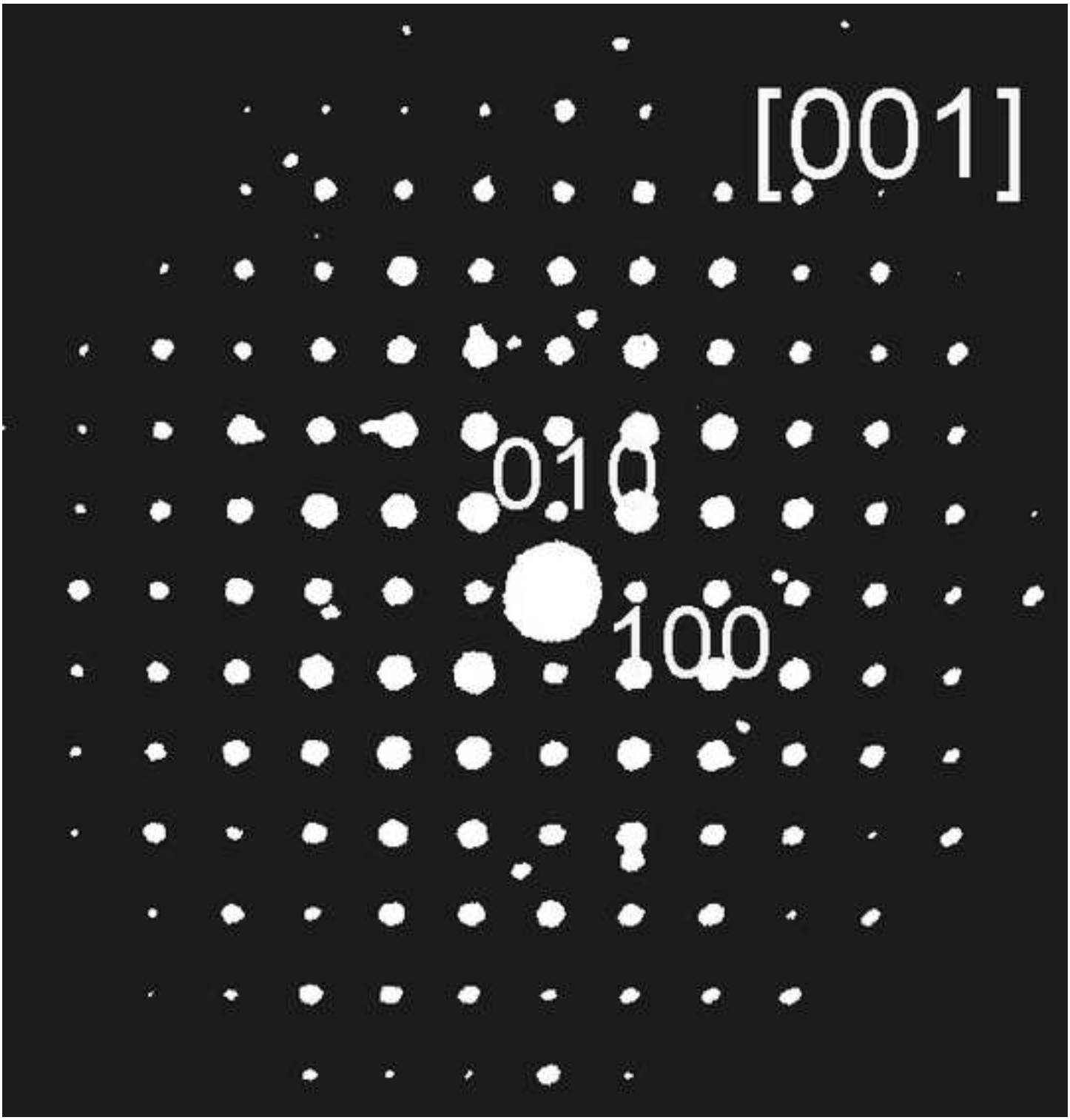

Figure

Click here to download high resolution image

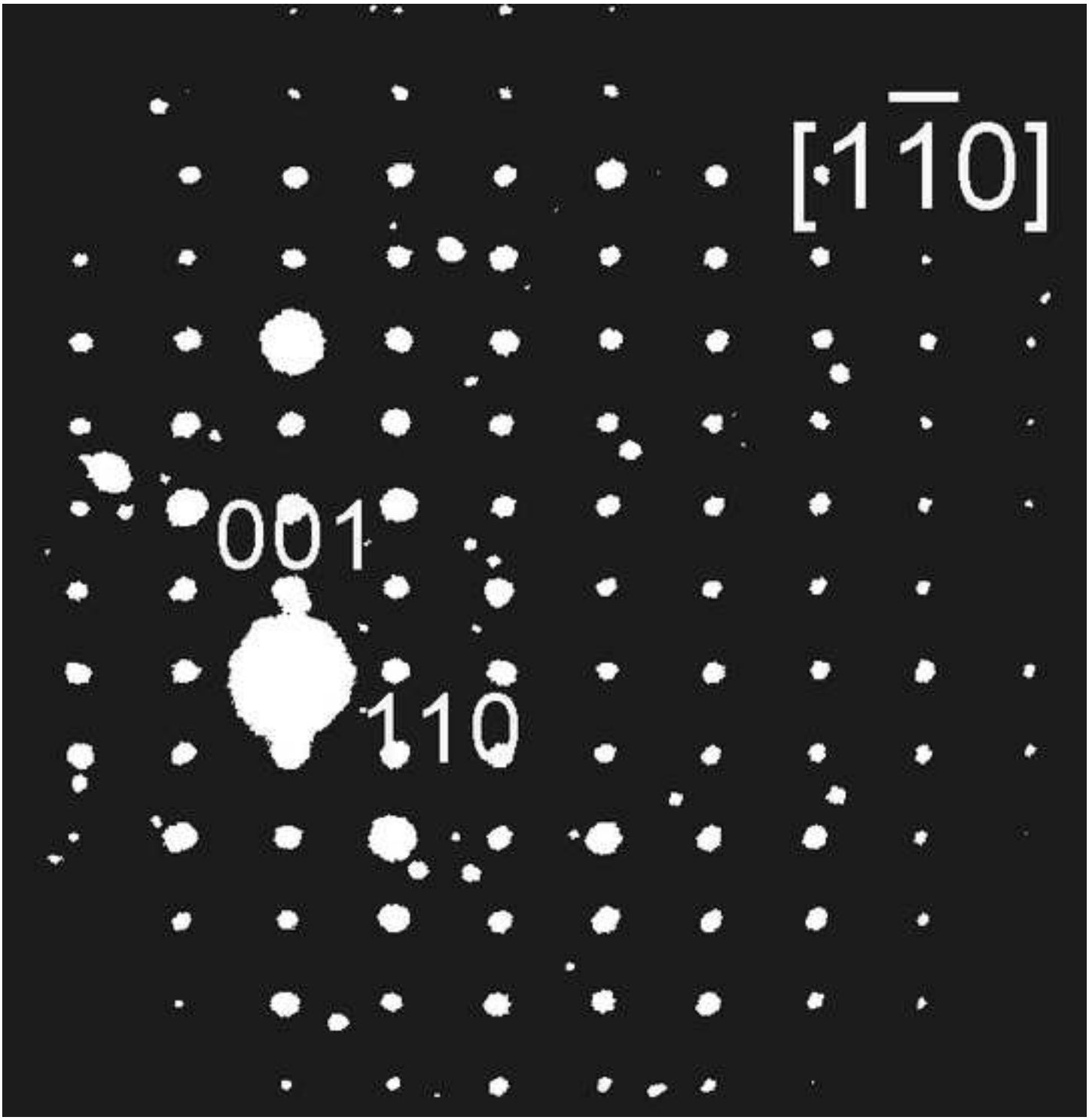

Figure

Click here to download high resolution image

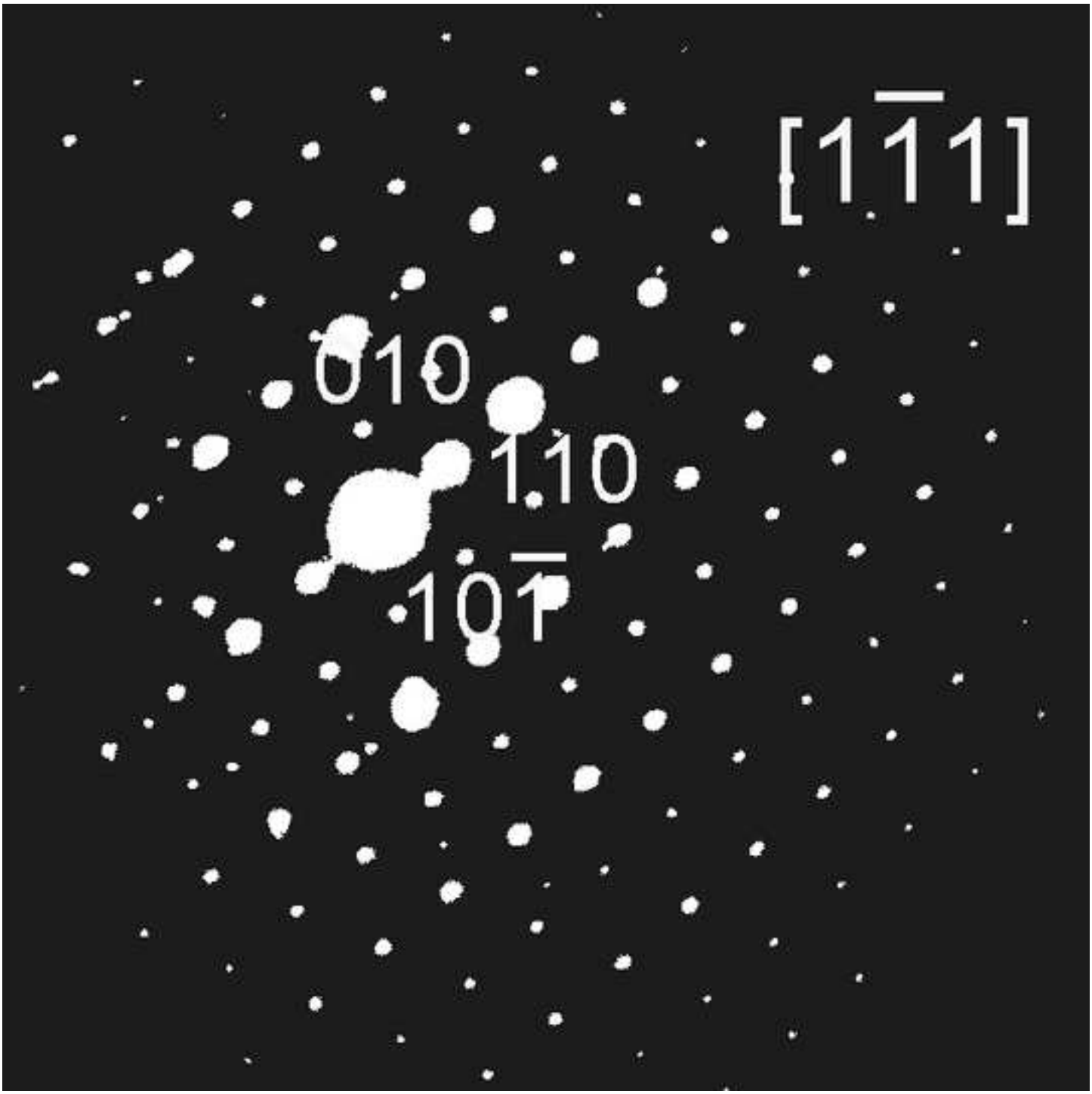

Figure

Click here to download high resolution image

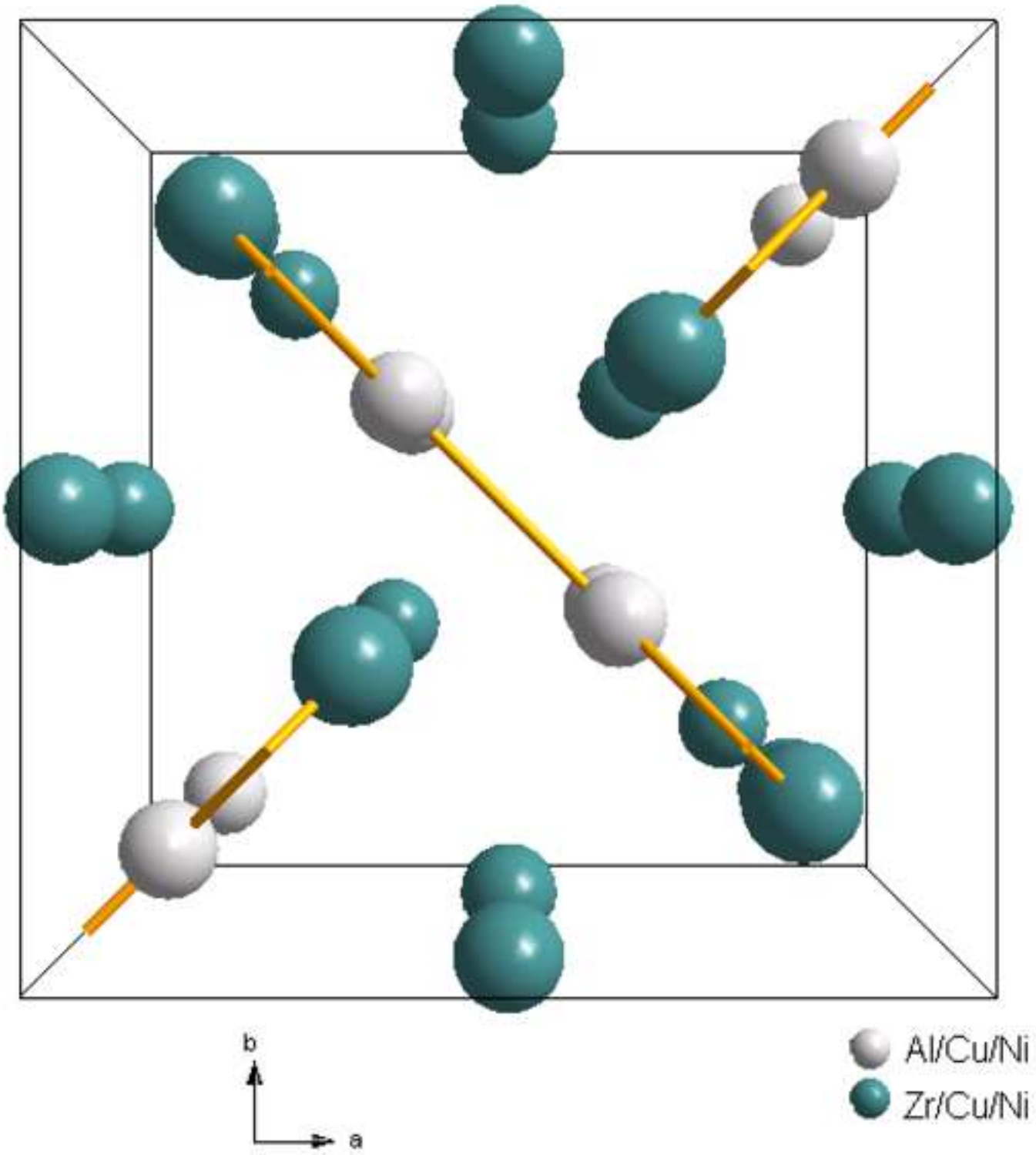

2016-08-21

In-situ structural identification of Zr3Al2 type metastable phase during crystallization of a Zr-based MG

Xing, Yan

Elsevier

Yan Xing, Yan Li, Xiangke Wang, Xiangtian Yu, Tao Zhang, Konstantinos Georgarakis, In-situ structural identification of Zr3Al2 type metastable phase during crystallization of a Zr-based MG, Journal of Non-Crystalline Solids, Volume 452, 15 November 2016, pp30-34

http://dx.doi.org/10.1016/j.jnoncrysol.2016.08.010